Top-down control of marine phytoplankton diversity in a global ecosystem model

A.E. Friederike Prowe [a,*], Markus Pahlow [a], Stephanie Dutkiewicz [b], Michael Follows [b], Andreas Oschlies [a]

[a] IFM–GEOMAR, Leibniz Institute of Marine Sciences at the University of Kiel, Düsternbrooker Weg 20, 24105 Kiel, Germany
[b] Department of Earth, Atmospheric, and Planetary Sciences, Massachusetts Institute of Technology, 77 Massachusetts Avenue, Cambridge, MA 02139, USA

ARTICLE INFO

ABSTRACT

The potential of marine ecosystems to adapt to ongoing environmental change is largely unknown, making prediction of consequences for nutrient and carbon cycles particularly challenging. Realizing that biodiversity might influence the adaptation potential, recent model approaches have identified bottom-up controls on patterns of phytoplankton diversity regulated by nutrient availability and seasonality. Top-down control of biodiversity, however, has not been considered in depth in such models. Here we demonstrate how zooplankton predation with prey-ratio based food preferences can enhance phytoplankton diversity in a ecosystem-circulation model with self-assembling community structure. Simulated diversity increases more than threefold under preferential grazing relative to standard density-dependent predation, and yields better agreement with observed distributions of phytoplankton diversity. The variable grazing pressure creates refuges for less competitive phytoplankton types, which reduces exclusion and improves the representation of seasonal phytoplankton succession during blooms. The type of grazing parameterization also has a significant impact on primary and net community production. Our results demonstrate how a simple parameterization of a zooplankton community response affects simulated phytoplankton community structure, diversity and dynamics, and motivates development of more detailed representations of top-down processes essential for investigating the role of diversity in marine ecosystems.

© 2011 Elsevier Ltd. All rights reserved.

1. Introduction

Evidence is increasing that biodiversity influences productivity and stability of ecosystems across trophic levels in both marine and terrestrial realms (Worm et al., 2006; Ptacnik et al., 2008). Theoretical considerations indicate that higher species richness can increase ecosystem stability (Tilman et al., 1997; Yachi and Loreau, 1999). However, experimental observations demonstrating diversity effects in marine pelagic ecosystems are scarce and the role of diversity for these ecosystems is not well known (Duffy and Stachowicz, 2006; Ptacnik et al., 2010). In light of anticipated changes in marine phytoplankton community structure (Moran et al., 2010; Boyd and Doney, 2002; Worm et al., 2002; Cardinale et al., 2006) and its effects on ecosystem structure and functioning (Bopp et al., 2005; Manizza et al., 2010), what shapes marine phytoplankton diversity is becoming a central research question.

Diversity is linked to differences in traits, e.g. optimal temperature for growth, within a community of species. One approach to capturing diversity in models is to formulate trade-offs between the different traits, which allows the system to emerge adaptively from environmental conditions (Norberg, 2004). This adaptive dynamics approach has been applied to models of local ecosystems

only (Bruggeman and Kooijman, 2007; Merico et al., 2009). On the global scale, prognostic models have made efforts to resolve some of the functional diversity of phytoplankton by increasing the number of plankton functional types (e.g. Le Quéré et al., 2005). With a stronger focus on traits, an alternative approach has employed an explicit community consisting of a large number of phytoplankton types (Follows et al., 2007) differing randomly in size, optimal temperature, growth parameters, and sinking speed (Section 2.1).

Recent studies using the Follows et al. (2007) model have demonstrated how distinct phytoplankton communities emerge in a global ocean model through bottom-up control by resource availability, where the emergent communities differed in their competitiveness for resources in different environments (Dutkiewicz et al., 2009; Barton et al., 2010). Besides bottom-up control, however, top-down mechanisms by consumers (predators) can shape diversity and ecosystem structure (Chesson, 2000; Worm et al., 2002; Chase et al., 2002). In models, structure and functioning of the simulated ecosystem are very sensitive to the choice of predation formulation (Anderson et al., 2010). In the previous studies based on the Follows et al. (2007) self-assembling ecosystem model, zooplankton predation was modeled in a simplistic way using two zooplankton types with similar Holling type II grazing responses and fixed preferences for each phytoplankton type. Here we show how a more flexible representation of the predation process can help

* Corresponding author. Tel.: +49 431 600 4032; fax: +49 431 600 4469.
E-mail address: fprowe@ifm-geomar.de (A.E.F. Prowe).

to better understand the emergence of phytoplankton diversity via top-down controls in a global ecosystem-circulation model.

2. Methods

2.1. The ecosystem model

The model used in this study is the Massachusetts Institute of Technology general circulation model (MITgcm) with the "Darwin" ecosystem module (Follows et al., 2007). The latter comprises prognostic equations of state for four nutrients (phosphorus, nitrogen, iron and silica), 78 phytoplankton types, one large and one small zooplankton type, dissolved and particulate organic matter. Phosphorus is used as the main currency of the model. Temperature-dependent phytoplankton growth takes into account limitation by light, including effects of self shading, and by a Liebig-type limitation by the most limiting nutrient according to a Michaelis–Menten formulation. Phytoplankton losses include a linear mortality, sinking and zooplankton predation, which is formulated as a Holling type II functional response. Both zooplankton types have the same maximum grazing rate and half-saturation concentration for grazing. Their grazing rates differ only in the preferences for the different phytoplankton types, which are assigned according to size and palatability. The export of organic matter to depth occurs mainly via particulate organic matter produced by phytoplankton mortality, sloppy feeding and zooplankton egestion and mortality. Sinking of phytoplankton plays a minor role. At the start of the simulation, the model ocean is seeded with the different phytoplankton types each characterized by a set of randomly assigned trait parameters. Phytoplankton types differ in cell size (small or large), nutrient requirements, half-saturation concentrations for nutrient uptake, light-limited growth, optimal temperature, and sinking speed (see Dutkiewicz et al. (2009) for equations and a detailed list of phytoplankton parameter ranges). The standard model setup in this study is identical to the one used by Dutkiewicz et al. (2009, Table A.1) except for a reduced zooplankton mortality (from $m^Z = 0.033$ d^{-1} to $m^Z = 0.013$ d^{-1}), which does not result in qualitative differences in diversity compared to the preceding studies. Three additional configurations employ modified predation formulations (see Sections 2.2 and 3.1, and Table 1). For each model configuration an ensemble of five integrations with different random phytoplankton parameter sets are performed. Here, we are using five of the random parameter sets also used by Dutkiewicz et al. (2009) for better comparability.

The physical model is forced offline by the ECCO-GODAE state estimates (Wunsch and Heimbach, 2007). The coupled ecosystem-circulation model is integrated on a global grid of 1° resolution with 24 depth levels for 10 years, by which time it mostly displays a repeating annual cycle in nutrients and primary production. Results are presented as the average of the ensemble of five integrations (see Appendix B, Fig. B.1), averaged over 0–55 m depth in the 10th year (unless noted otherwise).

2.2. High/low grazing configuration

The Holling type II predation formulation describes the grazing process in terms of two compound parameters, namely the maximum grazing rate (g_{max}) and the half-saturation concentration for grazing (κ_k^P), which by themselves cannot be directly interpreted in mechanistic terms. In this study, we investigate the sensitivity of the model results to changes in the grazing formulation by using two parameterizations characterized by high and low grazing rates (the *high grazing* and *low grazing* setups, respectively). For the *high grazing* setup, we derive g_{max} and κ_k^P from a size-based mechanistic feeding-strategy model describing encounter and capture between a suspension feeder and its immotile phytoplankton prey (see Appendix A for a detailed description). In the simplest configuration this mechanistic model reduces to a type II formulation that is structurally identical to the type II formulation used previously (Dutkiewicz et al., 2009; Barton et al., 2010). However, this approach allows us to determine g_{max} and κ_k^P from biologically meaningful parameters describing the grazing process. The mechanistic model results in notably higher g_{max} and lower κ_k^P than the original parameterization, and is thus referred to as *high grazing* setup in contrast to the *low grazing* standard configuration.

2.3. Diversity measures

We define the metric "diversity" to be the number of phytoplankton types that exceed a low threshold biomass concentration of $P_{th} = 10^{-8}$ mmol m^{-3} (in units of phosphorus; following Barton et al., 2010). Since phytoplankton types in the model are distinguished by functional traits such as maximum growth rates, the modeled functional diversity does not necessarily compare quantitatively to observational measures of (taxonomic) species richness. The modeled diversity depends to a limited extent on the number of phytoplankton types initialized (as indicated by related simulations with different numbers of phytoplankton types; Prowe et al., 2012) as well as on the chosen threshold concentration. Therefore

Table 1

Model configurations. Parameter values of maximum grazing rate (g_{max}) and half-saturation concentration for grazing (κ_k^P). Global annual average and maximum phytoplankton diversity as Shannon Index and as number of phytoplankton types exceeding threshold concentration P_{th} for $P_{th} = 10^{-8}$ mmol P m^{-3} (default), $P_{th} \times 10$ and $P_{th}/10$. Global annual average total phytoplankton biomass (0–55 m), primary production (PP) and net community production (NCP; both 0–100 m).

Configuration		LGNS low grazing and no switching	LGAS low grazing and active switching	HGNS high grazing and no switching	HGAS high grazing and active switching
Switching		No	Active	No	Active
κ_k^P	mmol P m^{-3}	0.1	0.1	0.027	0.027
g_{max}	d^{-1}	0.5	0.5	1.0	1.0
Ave. diversity	No. types	6.5	10.5	4.6	21.3
Ave. diversity ($P_{th} \times 10$)	No. types	5.8	9.4	4.1	19.1
Ave. diversity ($P_{th}/10$)	No. types	7.0	11.3	5.0	23.0
Max. diversity	No. types	15.9	37.4	10.4	55.3
Max. diversity ($P_{th} \times 10$)	No. types	14.3	35.0	9.1	52.2
Max. diversity ($P_{th}/10$)	No. types	16.9	38.8	11.1	59.4
Ave. Shannon Index		0.7	1.1	0.6	2.0
Max. Shannon Index		1.5	2.6	1.3	3.3
Ave. total phytoplankton	10^{-3} mmol P m^{-3}	8.4	11.5	1.92	5.7
Ave. PP	g C m^{-2} d^{-1}	0.18	0.21	0.09	0.16
Ave. NCP	g C m^{-2} d^{-1}	0.09	0.11	0.04	0.09

we also calculated the Shannon Index (H) from the biomass concentrations (P) of all phytoplankton types

$$H = -\sum_j^n p_j ln(p_j) \quad , \quad p_j = \frac{P_j}{\sum_r P_r}. \tag{1}$$

Though not intuitively related to ecological diversity, H considers the joint influence of species richness and evenness (Stirling and Wilsey, 2001) and takes into account all phytoplankton types without the need of a threshold concentration.

3. Grazing parameterizations

3.1. "No switching" and "active switching" configurations

In the standard configuration of the model (Dutkiewicz et al., 2009), the Holling type II formulation describes ingestion (I_{jk}) of phytoplankton type j by zooplankton type k depending on the biomass concentration of phytoplankton type j (P_j)

$$I_{jk} = g_{max} \frac{\rho_{jk} P_j}{\kappa_k^P + \sum_r \rho_{rk} P_r}. \tag{2}$$

Each of the two zooplankton types k is assigned different, but fixed preferences (ρ_{jk}) for each phytoplankton type j which are set to values between 0 and 1 according to the body sizes of both zooplankton and phytoplankton as well as the phytoplankton functional type (e.g. diatoms, prochlorococcus analogues).

This setup relies on the assumption that the impact of the entire grazer community can be represented by two functional types with fixed food preferences. An explicit representation of the predator community response would require adding a large number of state variables. Instead, we here parameterize the grazer community response implicitly by assuming that consumers covary with the resources on which they are specialized. Such a community response can be captured by replacing the fixed food preferences (ρ) by selectivities (σ), which are calculated from ρ and scaled by the biomass of each phytoplankton type j (Fasham et al., 1990) relative to total phytoplankton biomass available for grazing

$$\sigma_j = \frac{\rho_j P_j}{\sum_r \rho_r P_r}. \tag{3}$$

When a food type declines, the corresponding selectivity, and hence ingestion, decreases, while an increasing food type will be selected more strongly and thus suffer from more intense predation.

This grazing formulation is referred to as active switching (Gentleman et al., 2003), while constant food preferences imply no switching. Switching is an effective means for promoting coexistence (Hutson, 1984) and stability in simulated ecosystems (Murdoch and Oaten, 1975) and has been implemented in several ecosystem models (Fasham et al., 1990; Fasham et al., 1993; Aumont et al., 2003; Aumont and Bopp, 2006). At the same time, this formulation can cause total ingestion to decrease although total available food increases, which was thought to be unbiological behavior (Gentleman et al., 2003). A recent modeling approach demonstrates, however, how reduced ingestion rates at higher prey concentrations can arise from copepods switching feeding strategies in the face of predation risk (Mariani and Visser, 2010). Active switching between similar kinds of prey was observed in microzooplankton (see Strom et al., 2000) and copepods (Paffenhöfer, 1984). Copepods also actively switch between kinds of prey by shifting to different feeding strategies (Jonsson and Tiselius, 1990; Saiz and Kiørboe, 1995; Kiørboe et al., 1996). Here we interpret active switching not only as behavioral change of one predator type, but as a compound effect of the unresolved predator community.

3.2. Grazing pressure

The choice of the grazing formulation is known to determine the simulated dynamics of simple nutrient–phytoplankton–zooplankton (NPZ) systems. Density dependent phytoplankton growth or loss terms, which depend on the phytoplankton concentration with an exponent >1, as introduced by the active switching formulation, can promote coexistence of several phytoplankton types (Gross et al., 2009). Density independent formulations (exponent = 1), for example for the no switching formulation in our model, lead to competitive exclusion. For grazing formulations this criterion for coexistence mathematically implies a positive slope of the clearance rate, I/P, as a function of P. This measure can also be used to characterize the effect of grazing formulations on the stability of simple NPZ systems with one phytoplankton (Gentleman and Neuheimer, 2008). Here we employ this measure to better understand the effect of switching behavior on phytoplankton diversity in a multi-phytoplankton type system. Instead of the term "clearance rate", which refers to the volume of water which zooplankton would entirely clear of prey given a certain ingestion rate, we use the term "specific grazing pressure" for the same quantity to stress the effect of grazing on the phytoplankton.

The specific grazing pressure ($G_{jk} = I_{jk}/P_j$) of zooplankton k for each phytoplankton type j provides a measure of the strength of predation aside from effects of predator concentration. If preferences (ρ_{jk}) are constant, i.e. for no switching (Eq. (2)), it is given by

$$G_{jk} = \frac{I_{jk}}{P_j} = g_{max} \frac{\rho_{jk}}{\kappa_k^P + \sum_r \rho_{rk} P_r}. \tag{4}$$

For selectivities changing with phytoplankton concentration (Eq. (3)), i.e. for active switching, it is

$$G_{jk} = g_{max} \frac{\rho_{jk} P_j}{\kappa_k^P \sum_r \rho_{rk} P_r + \sum_r \rho_{rk} P_r^2}. \tag{5}$$

The slope of G_{jk} is calculated as the first derivative with respect to the phytoplankton concentration of type j ($\partial G_{jk}/\partial P_j$). For no switching, $\partial G_{jk}/\partial P_j$ is negative for all P_j

$$\frac{\partial G_{jk}}{\partial P_j} = -g_{max} \frac{\rho_{jk}^2}{\left(\kappa_k^P + \sum_r \rho_{rk} P_r\right)^2} < 0 \tag{6}$$

For active switching, $\partial G_{jk}/\partial P_j$ is given by

$$\frac{\partial G_{jk}}{\partial P_j} = g_{max} \frac{\rho_{jk}\left(\sum_{r \neq j} \rho_{rk} P_r^2 - \rho_{jk} P_j^2 + \kappa_k^P \sum_{r \neq j} \rho_{rk} P_r\right)}{\left(\sum_r \rho_{rk} P_r^2 + \kappa_k^P \sum_r \rho_{rk} P_r\right)^2} \tag{7}$$

and can be positive or negative depending on ρ_{rk} and P_j.

The initial slope at $P_j = 0$ can be calculated from

$$\frac{\partial}{\partial P_j}\left(\frac{I_{jk}}{P_j}\right)\bigg|_{P_j=0} = g_{max} \frac{\rho_{jk}\left(\sum_{r \neq j} \rho_{rk} P_r^2 + \kappa_k^P \sum_{r \neq j} \rho_{rk} P_r\right)}{\left(\sum_r \rho_{rk} P_r^2 + \kappa_k^P \sum_r \rho_{rk} P_r\right)^2} \tag{8}$$

$$\overset{P_j=0}{=} g_{max} \frac{\rho_{jk}}{\sum_r \rho_{rk} P_r^2 + \kappa_k^P \sum_r \rho_{rk} P_r} > 0 \tag{9}$$

and is always positive. This indicates that G_{jk} increases up to a critical phytoplankton concentration P_j^{crit} which can be determined by

$$\frac{\partial G_{jk}}{\partial P_j} = 0 \Longleftrightarrow P_j^{crit} = \sqrt{\frac{1}{\rho_{jk}}\left(\sum_{r \neq j} \rho_{rk} P_r^2 + \kappa_k^P \sum_{r \neq j} \rho_{rk} P_r\right)}. \tag{10}$$

For a sigmoidal type III grazing functional response, as used for instance by Yool et al. (2011), a similar result is obtained.

Active switching and no switching thus imply qualitatively different behavior when phytoplankton concentrations change.

Active switching can promote coexistence by damping changes in individual phytoplankton concentration as long as phytoplankton concentrations do not exceed P_j^{crit}. No switching may promote dominance of individual phytoplankton types because it amplifies changes in phytoplankton concentration. In the context of stability of NPZ models, a positive slope reduces oscillations and creates refuges from predation for the phytoplankton (Gentleman and Neuheimer, 2008). A negative slope causes a positive feed-back between phytoplankton concentration and growth and destabilizes the system. Below, we show that the slope of the grazing pressure can also explain how active switching helps to generate niches for less abundant phytoplankton types and thereby enhance phytoplankton diversity. We compare results of the active and the no-switching formulations (Section 3.1), each with low and high grazing rates from the original configuration and the mechanistic grazing model (Section 2.2), respectively, yielding four configurations: *low grazing and no switching* (LGNS), *low grazing and active switching* (LGAS), *high grazing and no switching* (HGNS), and *high grazing and active switching* (HGAS; Table 1).

4. Results and discussion

4.1. Phytoplankton diversity patterns

For LGNS (essentially the same as Barton et al. (2010)), phytoplankton diversity, measured as the number of types exceeding $P_{th} = 10^{-8}$ mmol P m^{-3}, averages 6.5 in the upper 55 m of the water column (Fig. 1a). Diversity increases by 62% to an average of 10.5 in LGAS (Fig. 1b). For HGAS, diversity rises more than threefold to an average of 21.3 (Fig. 1d). Simply increasing grazing rates, however, does not necessarily increase diversity as can be seen in HGNS for

which diversity decreases compared to LGNS to an average of 4.6 species present (Fig. 1c).

All configurations show low diversity at high latitudes, and higher diversity at low and intermediate latitudes (Figs. 2 and 3). Maximum zonal average diversity at around 45° latitude arises from hot spots in the western boundary currents (Barton et al., 2010), where waters with different phytoplankton types mix, thereby increasing local diversity. In these turbulent regions, vertical transport processes associated with frontal dynamics maintain a high nutrient supply to the surface ocean which can promote diversity by allowing both well and less well adapted phytoplankton types to grow. In the simulations with higher diversity, switching prevents weaker competitors from being excluded. Mixing of different water masses thus brings together even larger numbers of phytoplankton types, and the predator-mediated diversity increase is highest. In contrast, in the oligotrophic gyres, a number of phytoplankton types equally well adapted to low nutrient levels coexist (Barton et al., 2010) and switching enhances diversity only weakly.

Particularly for HGAS, the simulated latitudinal pattern of phytoplankton diversity appears broadly consistent with observational estimates along the Atlantic Meridional Transect (AMT; Fig. 2c; Cermeño et al., 2008). However, comparing simulated and observed diversity is not straight forward and any apparent agreement or disagreement might be coincidental. Maximum simulated diversity is obviously limited by the number of phytoplankton types with which the model is initialized. In addition, these results might be sensitive to the choice of the threshold concentration, P_{th}. The sensitivity with respect to P_{th} appears to be minor, since changing P_{th} by a factor of 10 results in diversity differences small compared to those due to switching (Fig. 2, Table 1). Observational estimates of the Shannon Index (H) along the AMT appear to be in
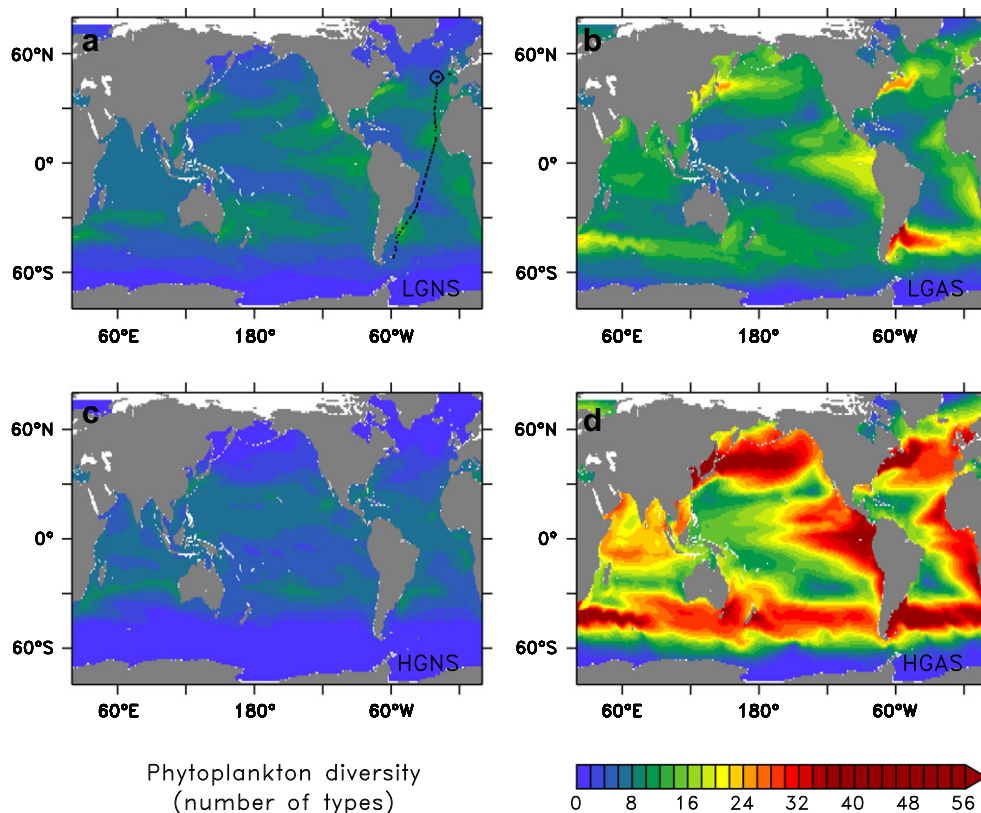

Fig. 1. Phytoplankton diversity. Annual average number of phytoplankton types exceeding a threshold concentration for (a), LGNS (b), LGAS (c), HGNS (d), HGAS. See Table 1 for abbreviations. The dots and circle in (a) mark the Atlantic Meridional Transect (AMT) and the site of the North Atlantic Bloom Experiment (NABE), respectively.
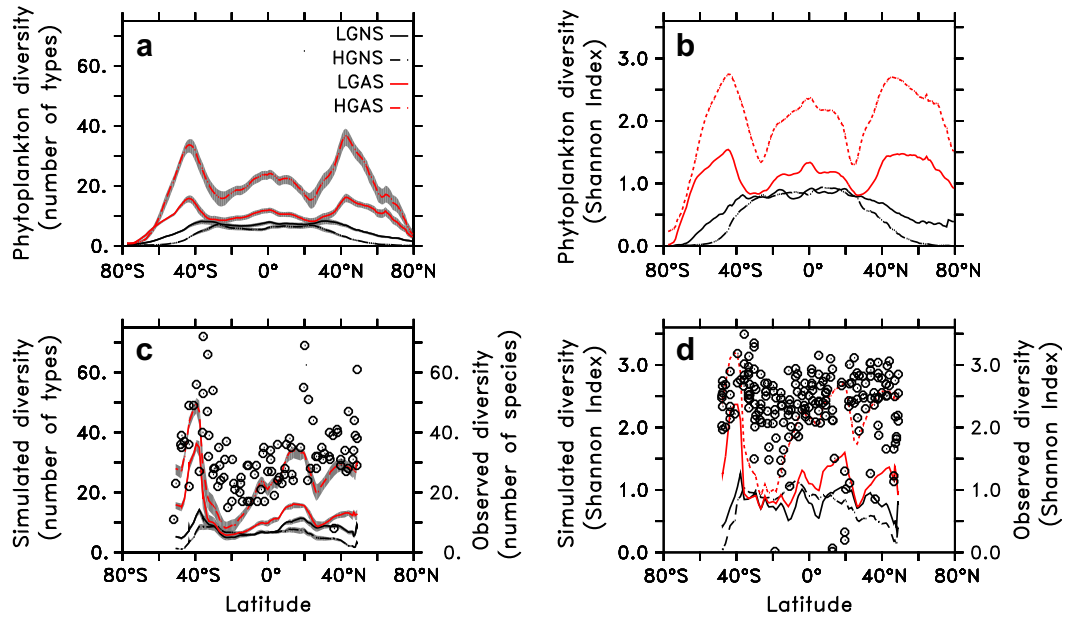
Fig. 2. Latitudinal diversity gradient. Simulated surface layer diversity as (a, c), number of phytoplankton types and (b, d) Shannon Index. Diversity is shown in (a, b) as zonal average and in (c, d) along the Atlantic Meridional Transect (AMT). Observed taxonomic diversity shown in (c, d) as number of species (surface data) and as Shannon Index (right y-axes) is calculated from biomass of diatoms, dinoflagellates and coccolithophores along the AMT (circles; Cermeño et al., 2008). Model estimates of functional diversity do not necessarily compare quantitatively to observational estimates of taxonomic diversity. Observational estimates of the Shannon Index may include data from the surface as well as from greater depths (P. Cermeño, personal communication). The uncertainty bands in (a) and (c) denote the diversity range between the ensemble averages of simulations with increased and decreased threshold concentration P_{th} compared to the standard configuration ($P_{th} \times 10$ and $P_{th}/10$, respectively).
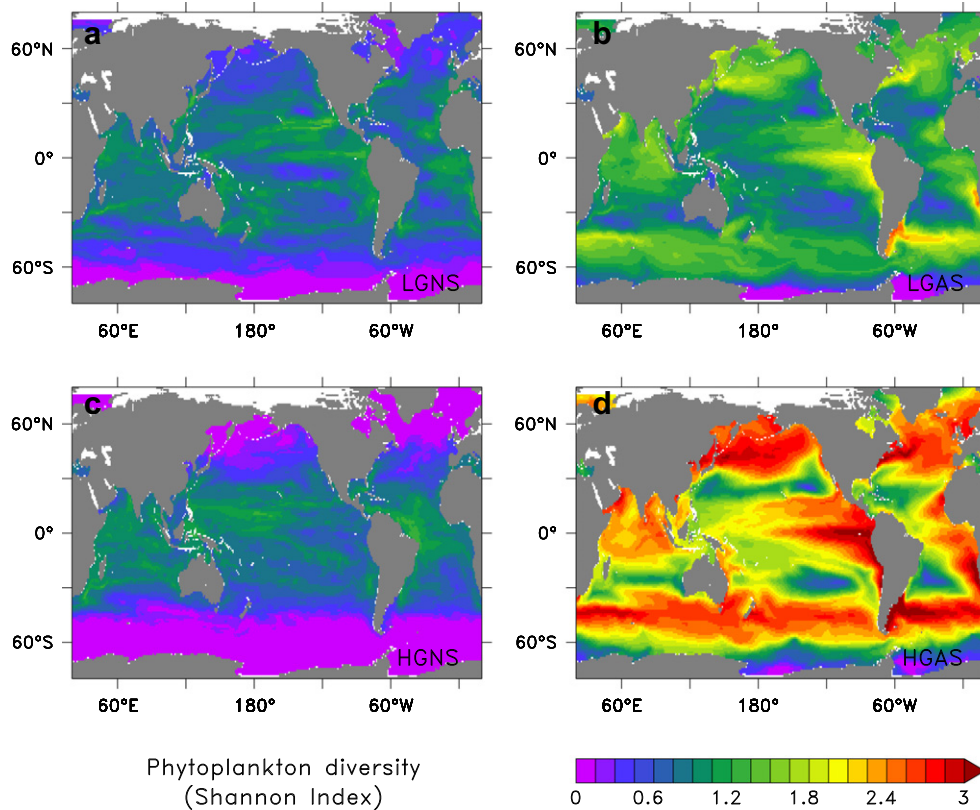

Fig. 3. Phytoplankton diversity. Annual average Shannon Index for (a), LGNS (b), LGAS (c), HGNS (d), HGAS. See Table 1 for abbreviations.

general higher than the simulations (Fig. 2d). No latitudinal gradient in H can be inferred from the observations along the AMT, possibly because these values include observations at different depths (Cermeño et al., 2008). In addition, both observational

diversity measures might be biased particularly at low latitudes since picophytoplankton were neglected (Aiken et al., 2009). This bias is, however, difficult to assess due to the unclear notion of "species" for this group.
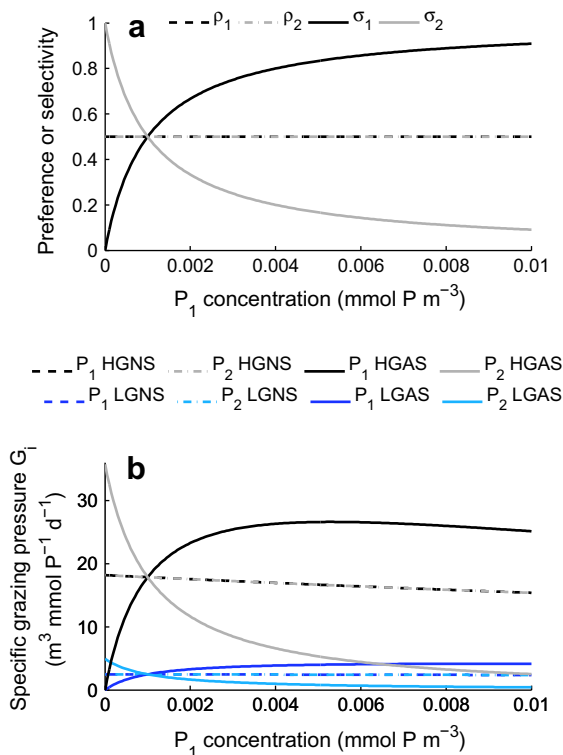
Fig. 4. Idealized two-phytoplankton system with equal preferences. (a) Preference (ρ) for *no switching* (dashed lines) or selectivity (σ) for *active switching* (solid lines). Phytoplankton P_1 increases from 0 to 0.01 mmol P m^{-3}, phytoplankton P_2 remains at 0.001 mmol P m^{-3}. (b) Corresponding specific grazing pressure for *high grazing* and *low grazing* (see Table 1 for parameter values).

4.2. Mechanisms of diversity increase

The mechanism by which active switching promotes phytoplankton diversity is illustrated by a simplified example with two equally preferred ($\rho_1 = \rho_2$) phytoplankton types. When the concentration of type 1 (P_1) increases from 0 to 0.01 mmol P m^{-3} with the concentration of type 2 (P_2) fixed at 0.001 mmol P m^{-3}, selectivity for type 1 (σ_1) increases with increasing P_1, while σ_2 decreases (Eq. (3), Fig. 4a). Increasing P_1 leads to higher specific grazing pressure (G_1) for small concentrations of P_1 as σ_1 increases, but reduces G_2 for the less abundant type P_2 by increasing total phytoplankton available for grazing ($\sum_r[\sigma_r P_r]$; Fig. 4b). In this example, when $P_1 > P_1^{crit}(= 0.006$ mmol P m^{-3}) any further increase of $\sum_r[\sigma_r P_r]$ leads to a reduction of G for both types. In contrast, under no switching, G for both types always decreases with increasing concentration of P_1 (Eq. (6)).

By increasing the specific grazing pressure on the most abundant phytoplankton types, active switching makes the less abundant types more competitive. The initial slope of G ($\partial G_{jk}/\partial P_j$) determines whether zooplankton predation can increase diversity in this way. For no switching, $\partial G_{jk}/\partial P_j$ is always negative (Eq. (6)) and therefore rewards growth of competitive types with reduced grazing pressure, thereby increasing competitiveness and promoting dominance of already successful types. In contrast, the active switching formulation has a positive initial slope at $P_j = 0$ (Eq. (9)) and G_{jk} thus increases if concentrations of type j increase up to a critical concentration (see Section 3.2), so that growth of this type is damped.

The strength of this increase in competitiveness is related to the initial slope of G and depends on the values of g_{max} and κ_k^P. For small g_{max} or large κ_k^P (compared to $\sum_r[\sigma_r P_r]$; LGAS) the initial slope is small (Fig. 4b) and the predator-mediated diversity increase is weaker than for HGAS (Fig. 1b and d). In contrast, no switching favors the most resource-competitive type by reducing specific grazing pressure with increasing concentration for all phytoplankton types and across all concentrations. In a model ecosystem with one phytoplankton, this reduction in grazing pressure with increasing phytoplankton biomass was shown to cause oscillations and thus reduces the stability of the system (Gentleman and Neuheimer, 2008). The same property of the grazing function tends to favor coexistence when applied to competing phytoplankton types. The variable grazing pressure creates additional limiting factors for each phytoplankton type individually and thereby enhances the number of competing phytoplankton types that can coexist (Levin, 1970; Chase et al., 2002). Switching thus constitutes
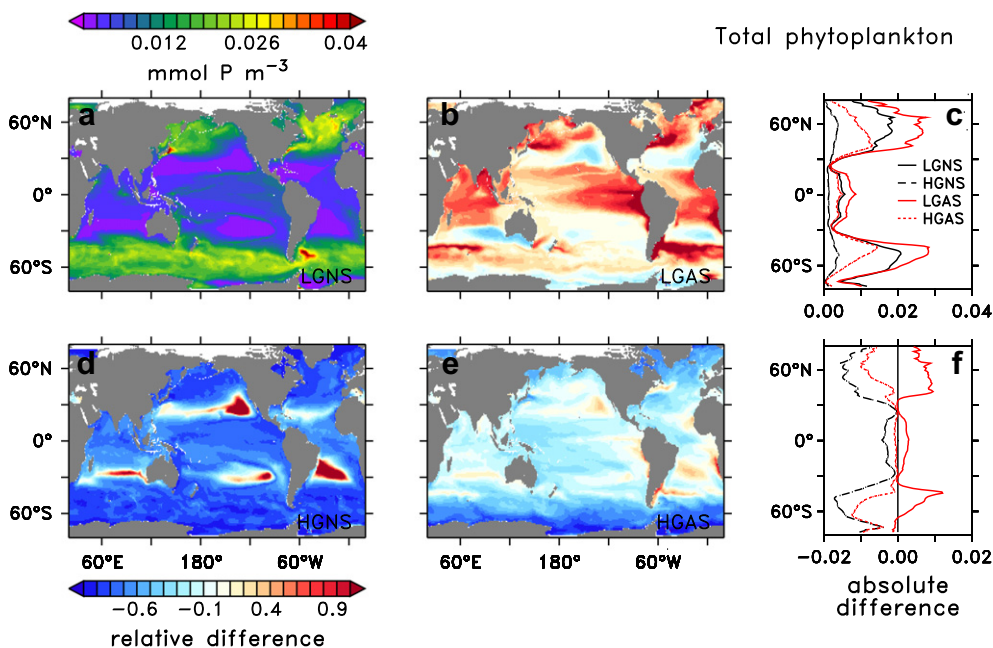

Fig. 5. Total phytoplankton biomass. (a) Annual average total phytoplankton biomass (0–55 m depth) for LGNS is compared to (b) LGAS, (d) HGNS, and (e) HGAS as relative difference to LGNS. Zonal averages of total phytoplankton biomass are shown in (c) as absolute values and in (f) as absolute difference to LGNS for all configurations.

one of many potential pathways (Roy and Chattopadhyay, 2007, and references therein) to resolve the "paradox of the plankton" (Hutchinson, 1961), which addresses the apparent contradiction between observed coexistence and theory predicting that the number of coexisting species cannot exceed the number of limiting factors (Levin, 1970).

4.3. Primary production and net community production

In the following, we discuss differences in simulated total phytoplankton biomass, primary production (PP) and net community production (NCP) between the different model configurations. NCP is defined as the difference between gross primary production and community respiration within the euphotic zone. Interestingly, NCP is not only controlled bottom-up by physical transport processes supplying nutrients, but it also changes in response to different grazing parameterizations. In fact, the total phytoplankton biomass, PP and NCP differ by as much as a factor of two in the annual mean among the different model simulations (Figs. 5–7; Table 1). The regional patterns of change relative to LGNS differ between both *low* and *high grazing* switching setups. The effects of switching can be seen when comparing LGAS to LGNS. A detailed
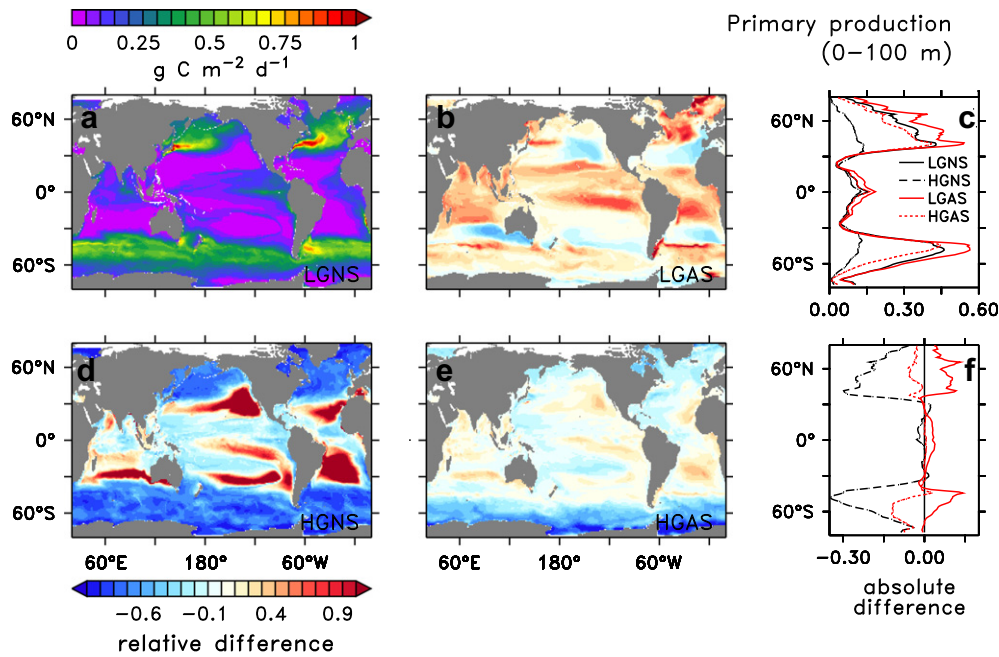

Fig. 6. Primary production (PP). (a) Annual average PP (0–100 m depth) for LGNS is compared to (b) LGAS, (d) HGNS, and (e) HGAS as relative difference to LGNS. Zonal averages of PP are shown in (c) as absolute values and in (f) as absolute difference to LGNS for all configurations.
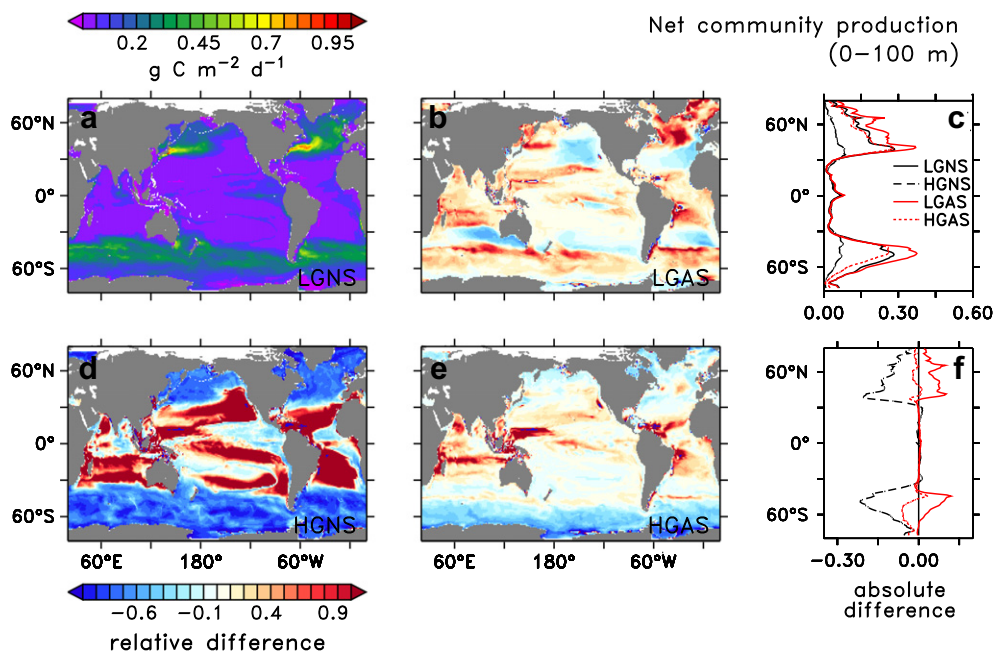

Fig. 7. Net community production (NCP). (a) Annual average NCP (0–100 m depth) for LGNS is compared to (b) LGAS, (d) HGNS, and (e) HGAS as relative difference to LGNS. Zonal averages of NCP are shown in (c) as absolute values and in (f) as absolute difference to LGNS for all configurations.

discussion of regional differences between configurations and the underlying mechanisms is presented in Appendix C. In the following, we summarize the main findings.

For both LGAS and HGAS, total phytoplankton biomass and PP increase compared to LGNS and HGNS, respectively, in the productive higher latitudes and in the tropics (shown for LGAS in Fig. 5b, Fig. 6b). For LGAS compared to LGNS, at higher latitudes higher uptake of nutrients intensifies the vertical nutrient gradients. It thereby enhances the mixing-driven input of nutrients from deeper layers which mostly fuels the PP increase. In combination with less grazing, higher phytoplankton biomass results, part of which is exported, thereby enhancing NCP. In contrast, in the permanently stratified low latitude regions (25°S–25°N) dominated by small phytoplankton types, higher total phytoplankton biomass enhances a "fast recycling loop" via dissolved organic matter (DOM) which sustains higher PP.

If grazing rates are increased (HGAS), a smaller phytoplankton standing stock leads to lower export, and thus lower NCP, in the productive regions. Less PP predominantly reflects lower nutrient inputs by vertical mixing. Opposing changes of PP and NCP in some regions (e.g., eastern tropical Atlantic and Pacific) indicate a reduction in community respiration. Less DOM production in the adjacent productive higher latitudes might reduce advective transport into these regions and thus decrease respiration. For HGNS, high grazing rates without switching generally reduce total phytoplankton biomass significantly compared to LGNS and increase nutrient concentrations with the exception of the subtropical gyres where total phytoplankton biomass is very small.

Our simulations demonstrate that a predator-mediated increase in phytoplankton diversity can coincide with an increase or a decrease in simulated productivity. An ecosystem with a more diverse phytoplankton community (LGAS) sustains higher PP and export production because of higher total phytoplankton biomass than a less diverse community (LGNS). However, this effect is sensitive to changes in model parameterization, as mechanisms that increase diversity can also result in lower productivity (HGAS).
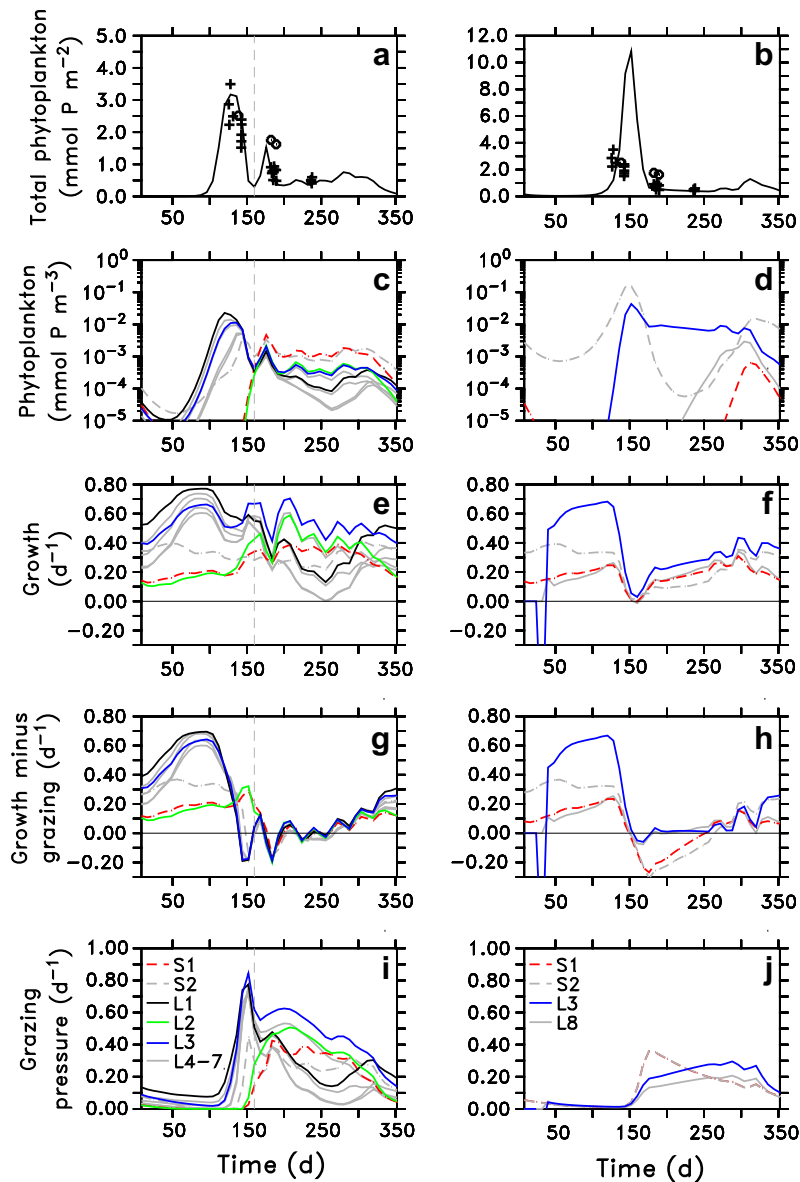

Fig. 8. Phytoplankton dynamics at the NABE site (47°N, 20°W). For HGAS (left) and LGNS (right) (a, b). Total phytoplankton concentration from simulations (line) and from observations of total phytoplankton biomass using C:P = 106 mol C (mol P)$^{-1}$ (circles) and of chlorophyll a using P:Chl = 0.7 g P (g Chl)$^{-1}$ (crosses). For all phytoplankton types present (S: small; L: large) averages of (c, d) concentrations, (e, f) growth (nutrient uptake minus sinking minus mortality), (g, h) growth minus grazing, and (i, j) total grazing pressure by both zooplankton types. Results are from a representative integration since specific phytoplankton composition differs between the five integrations of the ensemble.

Changes in productivity are fueled by differences in nutrient distributions relative to the standard configuration, and thus differ regionally depending on the physical regime. However, these differences reflect the state of the ecosystem after only short (10 year) integrations from the same initial conditions. Longer term adjustments within the ecosystem might modify the results.

The HGAS configuration reduces simulated differences in PP between eastern and western North Atlantic. This is potentially an improvement in the models results: Observational estimates of PP at BATS (Bermuda Atlantic Time-series Study site) and at ESTOC (European Station for Time series in the Ocean) show little difference (0.38 vs. 0.4 g C m^{-2} d^{-1}; Mouriño-Carballido and Neuer, 2008). On a global scale, however, the significance of the differences in PP and NCP is difficult to assess, as they are comparable with the uncertainties attached to the observational estimates. Differences in export production (not shown) between the different configurations are comparable to differences found for different multi-prey grazing formulations by Anderson et al. (2010). Our results support their study in confirming that multi-prey grazing functional responses have a large influence on simulated model dynamics. A more detailed comparison addressing phytoplankton community structure, specifically regarding the effect of explicitly representing phytoplankton diversity within plankton functional types, is to be reported elsewhere.

4.4. Seasonal phytoplankton dynamics

The seasonal pattern of simulated phytoplankton diversity is illustrated for the site of the North Atlantic Bloom Experiment (NABE), where active switching sustains a more diverse phytoplankton community. For HGAS, the first phytoplankton spring bloom is followed by a second, lower biomass peak and moderate concentrations for the remainder of the year (Fig. 8a). This double peak agrees well with observed phytoplankton biomass (converted from carbon to phosphorus units using C:P = 106 mol C (mol P)$^{-1}$ or from chlorophyll a data using P:Chl = 0.7 g P (g Chl)$^{-1}$). The first peak (days 100–150) is dominated by large phytoplankton types which had high winter biomass (types L1, L3 in Fig. 8c) and high growth rates (Fig. 8e) in their environment. However, the type with the highest concentration also feels the highest grazing pressure ($G \cdot Z$, Fig. 8i), which reduces its growth more strongly than that of other types (Fig. 8g) which then bloom consecutively. The second peak (day 175) is dominated by small phytoplankton types with lower maximum growth rates and higher nutrient affinity (S1, S2). Low grazing pressure allows them to survive the early spring and to finally displace the fast growing species (e.g. L1, L3) once nutrient concentrations decline at the end of the first bloom peak. This succession of smaller types following the larger types dominating the bloom is in good agreement with observations at NABE (Lochte et al., 1993; Sieracki et al., 1993).

The active switching formulation suggests that phytoplankton which achieve a biomass exceeding P_{crit} may benefit from reduced specific grazing pressure and thus potentially escape grazing control. The P_{crit} depends on the biomass of the other phytoplankton types (Eq. (10)) and is therefore a variable property of the phytoplankton community. In particular, if many phytoplankton types coexist and total biomass is high, it is more difficult for one type to exceed the higher P_{crit} than if total biomass is low. Furthermore, a concurrent increase in zooplankton biomass may offset a reduction in specific grazing pressure. Within the bloom dynamics in our model presented here, such effects are not immediately obvious.

In contrast to HGAS, the standard configuration (LGNS) produces only one bloom peak (Fig. 8b) with one dominating small and one large phytoplankton type (Fig. 8d; S2 and L3, respectively). It overestimates observed peak biomass by a factor of 3 for the conversion assumed (see caption of Fig. 8). Here again types with high winter

biomass (Fig. 8d) and high growth rates (Fig. 8f) dominate the peak. Without switching, grazing pressure is comparably high on all four phytoplankton types present until the bloom peak (Fig. 8j) and the types less adapted to winter conditions (S1, L8) cannot survive the bloom in sufficient concentrations to take over afterwards. As a consequence of the lower grazing pressure at high food concentrations, the bloom peaks later and is more pronounced for LGNS compared to HGAS. The bloom is ended bottom up by nutrient limitation on growth rates and top-down effects are of minor importance (Fig. 8f and h). For LGAS, results are between those for LGNS and HGAS: the model simulates seasonal succession of 3 types during the first bloom peak, but overestimates observed phytoplankton biomass and captures only one bloom peak. HGNS yields abrupt dynamics which seem unrealistic and overestimates observed phytoplankton biomass to a larger extent than does LGNS.

In previous modeling studies at NABE, the double peak was thought to result from co-limitation of diatoms by silicate (Fasham and Evans, 2000) or from single-phytoplankton-single-zooplankton interactions (Schartau and Oschlies, 2003). In our simulations with active switching, the double peak is a consequence of a phytoplankton community shift driven by both bottom-up and top-down mechanisms.

The simulated community dynamics at BATS mirror the differences from configurations at NABE. At BATS, the bloom is less clearly defined and total phytoplankton biomass is lower, but broadly consistent with chlorophyll observations. For HGAS, two bloom peaks are formed through a succession of large and small phytoplankton types, albeit less clearly than at NABE. For LGNS, one dominant phytoplankton type generates two less distinct bloom peaks. For both configurations, the bloom period is ended bottom-up by declining growth rates and top-down control by grazing is not important during this time of the year.

5. Conclusions

Our results indicate that grazing pressure can be a key factor in shaping phytoplankton succession and community structure during blooms. Prey-ratio based predation, e.g. a type III or active switching formulation, increases diversity and better captures the observed phytoplankton succession. Significant changes in primary and net community production occur between simulations with different grazing formulations. Regional differences highlight the role of recycling of organic matter in models. We have shown here top-down mechanisms to have the potential for being essential drivers of phytoplankton diversity in global ecosystem models. In addition to the ongoing attempts to relate phytoplankton diversity to physiological variances in the phytoplankton population, the intricate interplay between top-down and bottom-up controls on shaping marine phytoplankton diversity patterns will require more attention in future studies.

Appendix A. Derivation of the *high grazing* parameter set

The grazing parameters in the *high grazing* configuration are derived from a mechanistic predation model for zooplankton. The model is based on size-dependent encounter rate formulations (Visser, 2007) for a generic cruise or current feeder. Encounter rates (r_{kj}; see Table A.1 for symbols and units) between a zooplankton predator k and its phytoplankton prey j are calculated from the volume the predator can search given its detection area $\left(\pi R_{det.k}^2\right)$, its swimming velocity $\left(v_k^z\right)$, the phytoplankton sinking speed $\left(v_{snk,j}^P\right)$, the phytoplankton abundance $\left(N_j^P\right)$, and the selectivity (σ) or preference (ρ), here shown for no switching

Table A.1
Symbols used in the text and parameter values used with the mechanistic predation model to derive the *high grazing* parameter set. j and k denote specific phytoplankton and zooplankton types, respectively. Cell or body sizes are given as equivalent spherical diameter (ESD).

| Variable	Value	Unit	Description
ESD_s^P	1 μm	μm	Cell size (ESD) of small phytoplankton
ESD_l^P	10 μm	μm	Cell size (ESD) of large phytoplankton
ESD_s^Z	30 μm	μm	Body size (ESD) of small zooplankton
ESD_l^Z	300 μm	μm	Body size (ESD) of large zooplankton
G_{jk}		mmol P^{-1} d^{-1}	Specific grazing pressure of zooplankton k for phytoplankton j
g_{max}	0.5 or 1	d^{-1}	Maximum grazing rate (small and large zooplankton)
I_{jk}		d^{-1}	Ingestion rate of zooplankton k for phytoplankton j
κ_s^P	0.1 or 0.027	mmol P m^{-3}	Half-saturation concentration for grazing (small zooplankton)
κ_l^P	0.1 or 0.027	mmol P m^{-3}	Half-saturation concentration for grazing (large zooplankton)
M_j^P		mmol P cell^{-1}	Phytoplankton body mass
M_k^Z		mmol P pred^{-1}	Zooplankton body mass
m^Z	0.0125	d^{-1}	Zooplankton mortality rate
N_j^P		cells m^{-3}	Phytoplankton abundance
P_j		mmol P m^{-3}	Phytoplankton concentration
$R_{det,k}$	1 ESD_k^Z	m	Zooplankton detection distance
r_{jk}		cells pred^{-1} d^{-1}	Encounter rate of zooplankton k and phytoplankton j
ρ_{jk}			Preference of zooplankton k for phytoplankton j
σ_{jk}			Selectivity of zooplankton k for phytoplankton j
t_H		d	Handling time
t_H^0	8×10^4 s	d	Handling time constant
$v_{snk,j}^P$		m d^{-1}	Phytoplankton sinking speed
v_k^Z	2.9 ESD_k^Z s^{-1}	m d^{-1}	Zooplankton swimming speed
V_j^P		μm^3	Phytoplankton cell volume (from ESD)
V_k^Z		μm^3	Zooplankton body volume (from ESD)
Z_k		mmol P m^{-3}	Zooplankton concentration
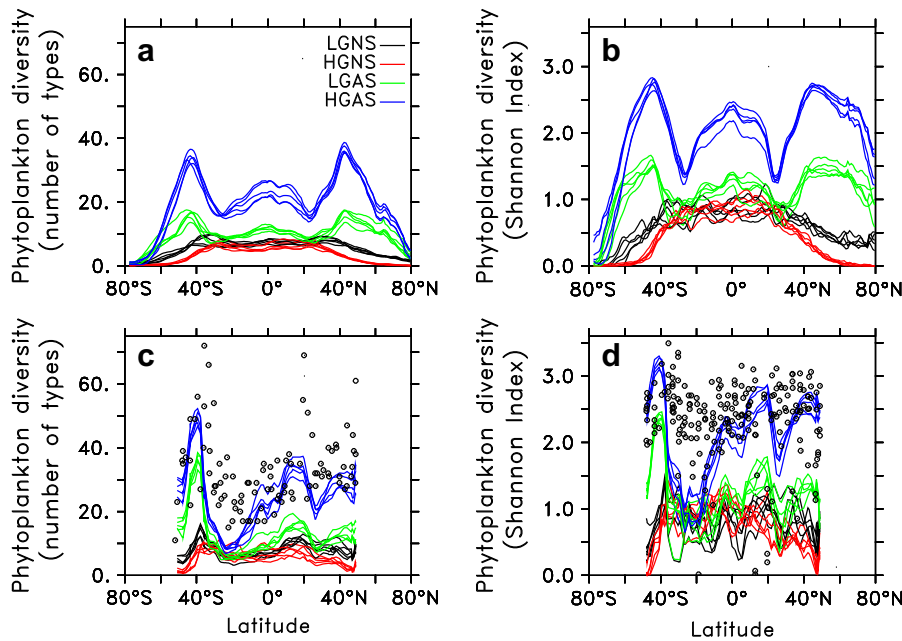
Fig. B.1. Diversity in individual integrations of the ensemble. Simulated annual average phytoplankton diversity as (a, c) number of phytoplankton types exceeding a threshold concentration of $P_{th} = 10^{-8}$ mmol P m^{-3} and (b, d) as Shannon Index. The ensemble of five integrations for LGNS, LGAS, HGNS, and HGAS is presented (a, b) as zonal average and (c, d) along the Atlantic Meridional Transect (AMT) in comparison to diversity calculated from biomass observations for diatoms, dinoflagellates and coccolithophores (circles) along the AMT as number of species (surface data) and Shannon Index (Cermeño et al., 2008).

$$r_{kj} = \pi R_{det,k}^2 \rho_{jk} N_j^P \sqrt{v_k^{Z\,2} + v_{snk,j}^{P\,2}}. \tag{A.1}$$

Detection distance ($R_{det,k}$) and v_k^Z are assumed to scale linearly with predator size (expressed as equivalent spherical diameter ESD_k^Z). The $v_{snk,j}^P$ are interpolated from observations (Smayda, 1970).

The ingestion rate is calculated from the encounter rates considering a handling time (t_H) per successful encounter between predator and prey

$$I_{jk} = \frac{M_j^P}{M_k^Z} \frac{r_{kj}}{1 + t_H r_{kj}}. \tag{A.2}$$

The handling time is set by the handling time constant (t_H^0) and assumed to vary proportionally with the predator–prey size ratio (M_j^P/M_k^Z; Pahlow and Prowe, 2010)

$$t_H = t_H^0 M_j^P / M_k^Z. \tag{A.3}$$

Effects of turbulence, in the form of an additional turbulent velocity increasing the encounter rates, are not considered here to enhance comparability with the original predation model.

The mechanistic predation model (Eqs. (A.1), (A.2)) reduces to a type II formulation for both active and no switching, here shown for no switching

$$I_{jk} = \frac{1}{t_{H_0}} \frac{\rho_{jk} P_j}{\frac{M_k^Z}{t_{H_0} F} + \rho_{jk} P_j}, \tag{A.4}$$

where $F = \pi R_{det,k}^2 \sqrt{v_k^{Z\,2} + v_{snk,j}^{P\,2}}$. The maximum ingestion rate is given by $g_{max} = 1/t_{H_0}$ and the half-saturation concentration is $\kappa_k^P = M_k^Z/(t_{H_0} F)$. This qualitatively corresponds to the traditional grazing formulation implemented in the original model (Eq. (2)).

Parameters for the mechanistic predation model were estimated from literature data. Zooplankton swimming speed generally increases with body size. For this application, $v_k^Z = 2.9\,ESD_k^Z$ s^{-1} according to data on different zooplankton groups ranging from 4 μm ESD to 1.3 mm ESD (Hansen et al., 1997; Broglio et al., 2001; Strom and Morello, 1988; Tiselius and Jonsson, 1990). The t_{H_0} is set to yield a maximum ingestion rate of about 1 d^{-1} (Hansen et al., 1997), which is used for both the small and the large zooplankton type to be consistent with the original model. Body masses of phytoplankton and zooplankton (M_j^P and M_k^Z,
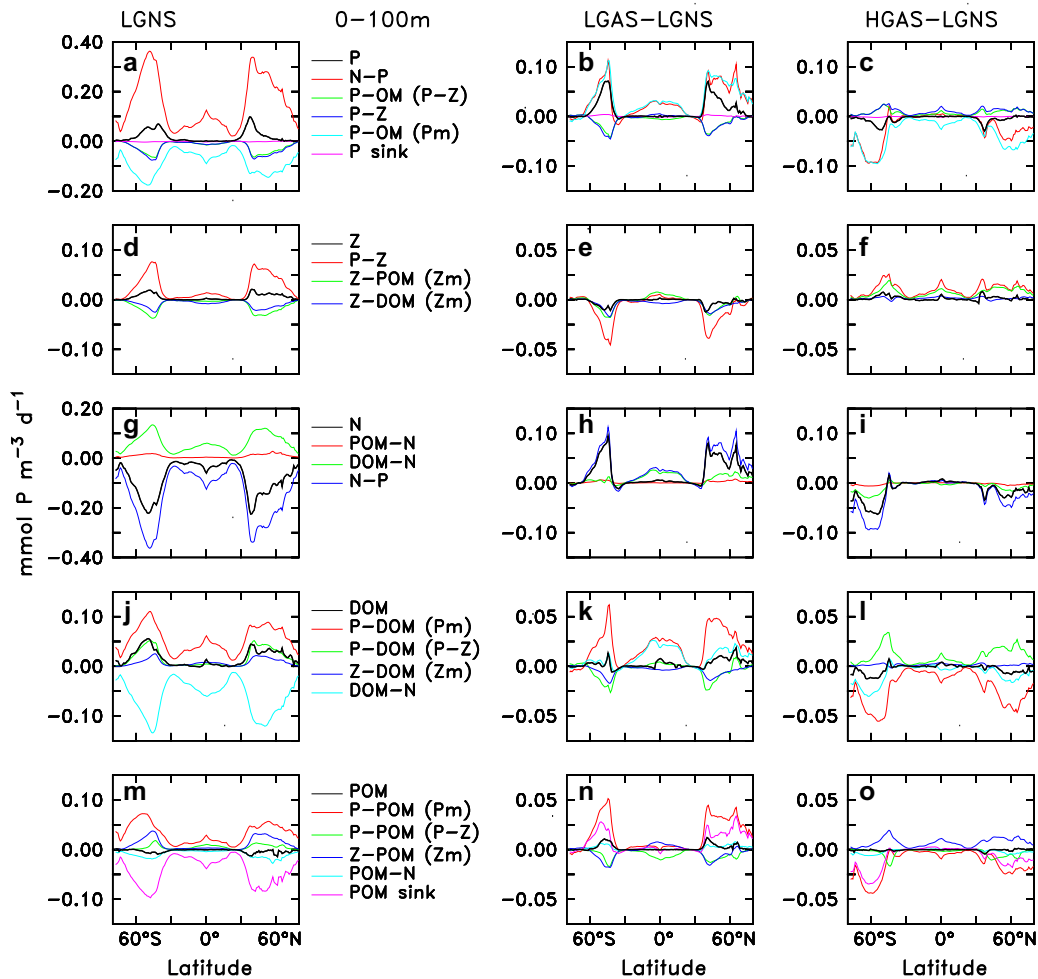

Fig. C.1. Differences in model dynamics between configurations. Fluxes between state variables in the model are shown integrated over the top 100 m as zonal average. Left panels: For LGNS, the black line represents the balance between source (positive) and sink (negative) fluxes. For LGAS and HGAS (middle and right panels, respectively), all lines are absolute changes relative to LGNS, with positive and negative values denoting increases and decreases of the respective flux. State variables for which fluxes are presented from top to bottom are phytoplankton (P), zooplankton (Z), nutrient (phosphate; N), dissolved organic matter (DOM) and particulate organic matter (POM). Fluxes are primary production (N-P), sloppy feeding losses (P-OM (P-Z)), grazing (P-Z), phytoplankton mortality (P-OM (Pm)), phytoplankton sinking (P sink), zooplankton losses to DOM (Z-DOM (Zm)) and POM (Z-POM (Zm)), recycling of DOM (DOM-N) and POM (POM-N) from phytoplankton mortality (P-DOM (Pm) and P-POM (Pm)) and sloppy feeding (P-DOM (P-Z) and P-POM (P-Z)), sinking of POM (POM sink). The black line in g shows that nutrients taken up by phytoplankton cannot be supplied by recycling of DOM and POM, and thus indicate physical supply by mixing.

respectively) are calculated from volumes (V_j^P and V_k^Z, respectively) based on cell or body size (ESD) for phytoplankton (Menden-Deuer and Lessard, 2000)

$$M_j^P \; [\text{pg C}] = 0.288 \cdot V_j^P \; [\mu m^3]^{0.811} \tag{A.5}$$

and for zooplankton (Verity and Langdon, 1984)

$$M_k^Z \; [\text{pg C}] = 0.445 + 0.053 \cdot V_k^Z \; [\mu m^3] \tag{A.6}$$

and converted to model units (mmol P cell^{-1}) using Redfield stoichiometry. The detection distance is set to $R_{det,k} = 1ESD_k^Z$ for simplicity, which is within the range of values calculated for hydromechanical detection of different types of prey (Visser, 2001). While for the *low grazing* configurations $g_{max} = 0.5 \, \text{d}^{-1}$ and $\kappa_k^P = 0.1$ mmol P m^{-3} (Table 1), the above parameter choices for the mechanistic model imply $g_{max} = 1 \, \text{d}^{-1}$ and $\kappa_k^P = 0.027$ mmol P m^{-3}, thus generally resulting in higher ingestion rates in the *high grazing* configurations. Differences in κ_k^P arising from the different size of the two zooplankton types (cf. Table A.1) are negligible and an intermediate κ_k^P is employed for both zooplankton types in accordance with the original model.

Appendix B. Diversity between different integrations of the ensemble

Results presented in this study are the average of an ensemble of five integrations each with a different set of phytoplankton parameters randomly chosen within a given range. Phytoplankton diversity differs only slightly between different integrations (Fig. B.1). The geographical patterns for all integrations (not shown) are similar and differ less between integrations with the same configuration than between different configurations.

Appendix C. Changes in primary production and net community production between configurations

For both LGAS and HGAS, total phytoplankton biomass and PP increase compared to LGNS and HGNS, respectively, in the productive higher latitudes and in the tropics (shown for LGAS in Fig. 5b, Fig. 6b). For LGAS, in higher latitudes lower nutrient concentrations in the surface mixed layer (not shown) lead to a stronger vertical nutrient gradient, and thereby cause higher input of nutrients from the deeper layers by processes like deep winter mixing (Fig. C.1h). This enhanced nutrient input fuels the largest part of the PP increase, while only a small fraction is due to higher recycling of dissolved organic matter (DOM). Together with less grazing (Fig. C.1e), higher total phytoplankton biomass remains (Fig. C.1b). In contrast, in the permanently stratified low latitude regions (25°S–25°N) with little nutrient input by vertical eddy diffusion, enhanced recycling of DOM via phytoplankton mortality is mostly responsible for higher PP and appears to enhance a "fast recycling loop" (Fig. C.1h). With switching, the damped growth of dominant types and the reduced grazing pressure on phytoplankton types less successful in the competition for nutrients allows the latter types to grow, albeit slowly, at low nutrient concentrations. This increases not only diversity, but also total phytoplankton biomass. At higher latitudes, a fraction of this phytoplankton biomass is exported to greater depths as particulate organic matter (POM; Fig. C.1n) which is thus not available for remineralization in the surface layer but enhances NCP instead (Fig. 7). The lower latitudes are dominated by small phytoplankton types, for which higher mortality leads to more DOM but little more POM (Figs. C1k and n). If grazing rates are increased (HGAS), the phytoplankton standing stock is reduced compared to LGAS, causing lower recycling of nutrients via phytoplankton mortality (Fig. C1c). The simultaneous decrease in PP, however, predominantly reflects lower nutrient inputs by vertical mixing caused by higher nutrient concentrations in the surface layer (Fig. C.1i). Lower phytoplankton mortality also leads to lower export of POM, and thus lower NCP (Fig. 7), in the productive regions, and is only partly compensated by increased fecal pellet production by the zooplankton (Fig. C.1o).

References

Aiken, J., Pradhan, Y., Barlow, R., Lavender, S., Poulton, A., Holligan, P., Hardman-Mountford, N., 2009. Phytoplankton pigments and functional types in the Atlantic Ocean: a decadal assessment, 1995–2005. Deep-Sea Research Part II – Topical Studies In Oceanography 56, 899–917.

Anderson, T.R., Gentleman, W.C., Sinha, B., 2010. Influence of grazing formulations on the emergent properties of a complex ecosystem model in a global Ocean general circulation model. Progress in Oceanography 87, 201–213.

Aumont, O., Bopp, L., 2006. Globalizing results from Ocean in situ iron fertilization studies. Global Biogeochemical Cycles 20. doi:10.1029/2005GB002591.

Aumont, O., Maier-Reimer, E., Blain, S., Monfray, P., 2003. An ecosystem model of the global Ocean including Fe, Si, P colimitations. Global Biogeochemical Cycles 17. doi:10.1029/2001GB001745.

Barton, A.D., Dutkiewicz, S., Flierl, G., Bragg, J., Follows, M.J., 2010. Patterns of diversity in marine phytoplankton. Science 327, 1509–1511.

Bopp, L., Aumont, O., Cadule, P., Alvain, S., Gehlen, M., 2005. Response of diatoms distribution to global warming and potential implications: A global model study. Geophysical Research Letters 32. doi:10.1029/2005GL023653.

Boyd, P., Doney, S., 2002. Modelling regional responses by marine pelagic ecosystems to global climate change. Geophysical Research Letters 29. doi:10.1029/2001GL014130.

Broglio, E., Johansson, M., Jonsson, P.R., 2001. Trophic interaction between copepods and ciliates: Effects of prey swimming behavior on predation risk. Marine Ecology Progress Series 220, 179–186.

Bruggeman, J., Kooijman, S.A.L.M., 2007. A biodiversity-inspired approach to aquatic ecosystem modeling. Limnology and Oceanography 52, 1533–1544.

Cardinale, B.J., Srivastava, D.S., Duffy, J.E., Wright, J.P., Downing, A.L., Sankaran, M., Jouseau, C., 2006. Effects of biodiversity on the functioning of trophic groups and ecosystems. Nature 443, 989–992.

Cermeño, P., Marañón, E., Harbour, D., Figueiras, F.G., Crespo, B.G., Huete-Ortega, M., Varela, M., Harris, R.P., 2008. Resource levels, allometric scaling of population abundance, and marine phytoplankton diversity. Limnology and Oceanography 53, 312–318.

Chase, J., Abrams, P., Grover, J., Diehl, S., Chesson, P., Holt, R., Richards, S., Nisbet, R., Case, T., 2002. The interaction between predation and competition: a review and synthesis. Ecology Letters 5, 302–315.

Chesson, P., 2000. Mechanisms of maintenance of species diversity. Annual Review of Ecology and Systematics 31, 343–366.

Duffy, J., Stachowicz, J., 2006. Why biodiversity is important to Oceanography: potential roles of genetic, species, and trophic diversity in pelagic ecosystem processes. Marine Ecology Progress Series 311, 179–189.

Dutkiewicz, S., Follows, M.J., Bragg, J.G., 2009. Modeling the coupling of Ocean ecology and biogeochemistry. Global Biogeochemical Cycles 23. doi:10.1029/2008GB003405.

Fasham, M., Ducklow, H., McKelvie, S., 1990. A nitrogen-based model of plankton dynamics in the Oceanic mixed layer. Journal of Marine Research 48, 591–639.

Fasham, M., Sarmiento, J., Slater, R., Ducklow, H., Williams, R., 1993. Ecosystem behavior at Bermuda Station-S and Ocean Weather Station India - A General-circulation model and observational analysis. Global Biogeochemical Cycles 7, 379–415.

Fasham, M.J.R., Evans, G.T., 2000. Advances in ecosystem modelling within JGOFS. In: Hanson, R.B., Ducklow, H.W., Field, J.G. (Eds.), The Changing Ocean Carbon Cycle. Cambridge University Press, pp. 417–446.

Follows, M.J., Dutkiewicz, S., Grant, S., Chisholm, S.W., 2007. Emergent biogeography of microbial communities in a model Ocean. Science 315, 1843–1846.

Gentleman, W., Leising, A., Frost, B., Strom, S., Murray, J., 2003. Functional responses for zooplankton feeding on multiple resources: A review of assumptions and biological dynamics. Deep-Sea Research Part II 50, 2847–2875.

Gentleman, W.C., Neuheimer, A.B., 2008. Functional responses and ecosystem dynamics: How clearance rates explain the influence of satiation, food-limitation and acclimation. Journal of Plankton Research 30, 1215–1231.

Gross, T., Edwards, A.M., Feudel, U., 2009. The invisible niche: Weakly density-dependent mortality and the coexistence of species. Journal of Theoretical Biology 258, 148–155.

Hansen, P.J., Bjørnsen, P.K., Hansen, B.W., 1997. Zooplankton grazing and growth: Scaling within the 2-2,000-µm body size range. Limnology and Oceanography 42, 687–704.

Hutchinson, G.E., 1961. The paradox of the plankton. The American Naturalist 95, 137–145.

Hutson, V., 1984. Predator mediated coexistence with a switching predator. Mathematical Biosciences 68, 233–246.

Jonsson, P.R., Tiselius, P., 1990. Feeding behaviour, prey detection and capture efficiency of the copepod *Acartia tonsa* feeding on planktonic ciliates. Marine Ecology Progress Series 60, 35–44.

Kiørboe, T., Saiz, E., Viitasalo, M., 1996. Prey switching behaviour in the planktonic copepod *Acartia tonsa*. Marine Ecology Progress Series 143, 65–75.

Le Quéré, C., Harrison, S., Prentice, I., Buitenhuis, E., Aumont, O., Bopp, L., Claustre, H., Cotrim Da Cunha, L., Geider, R., Giraud, X., Klaas, C., Kohfeld, K., Legendre, L., Manizza, M., Platt, T., Rivkin, R., Sathyendranath, S., Uitz, J., Watson, A., Wolf-Gladrow, D., 2005. Ecosystem dynamics based on plankton functional types for global Ocean biogeochemistry models. Global Change Biology 11, 2016–2040.

Levin, S.A., 1970. Community equilibria and stability, and an extension of the competitive exclusion principle. American Naturalist 104, 413–423.

Lochte, K., Ducklow, H., Fasham, M., Stienen, C., 1993. Plankton succession and carbon cycling at 47°N-20°W during the JGOFS North-Atlantic Bloom Experiment. Deep-Sea Research Part II – Topical Studies In Oceanography 40, 91–114.

Manizza, M., Buitenhuis, E.T., Le Quéré, C., 2010. Sensitivity of global Ocean biogeochemical dynamics to ecosystem structure in a future climate. Geophysical Research Letters 37. doi:10.1029/2010GL043360.

Mariani, P., Visser, A.W., 2010. Optimization and emergence in marine ecosystem models. Progress in Oceanography 84, 89–92.

Menden-Deuer, S., Lessard, E.J., 2000. Carbon to volume relationships for dinoflagellates, diatoms, and other protist plankton. Limnology and Oceanography 45, 569–579.

Merico, A., Bruggeman, J., Wirtz, K., 2009. A trait-based approach for downscaling complexity in plankton ecosystem models. Ecological Modelling 220, 3001–3010.

Morán, X.A.G., López-Urrutia, A., Calvo-Díaz, A., Li, W.K.W., 2010. Increasing importance of small phytoplankton in a warmer Ocean. Global Change Biology 16, 1137–1144.

Mouriño-Carballido, B., Neuer, S., 2008. Regional differences in the role of eddy pumping in the North Atlantic Subtropical Gyre – historical conundrums revisited. Oceanography 21, 52–61.

Murdoch, W.W., Oaten, A., 1975. Predation and population stability. Advances in Ecological Research 9, 1–131.

Norberg, J., 2004. Biodiversity and ecosystem functioning: A complex adaptive systems approach. Limnology and Oceanography 49, 1269–1277.

Paffenhöfer, G.A., 1984. Food ingestion by the marine planktonic copepod *Paracalanus* in relation to abundance and size distribution of food. Marine Biology 80, 323–333.

Pahlow, M., Prowe, A.E.F., 2010. Model of zooplankton optimal current feeding. Marine Ecology Progress Series 403, 129–144.

Prowe, A.E.F., Pahlow, M., Oschlies, A., 2012. Controls on the diversity-productivity relationship in a marine ecosystem model. Ecological Modelling 225, 167–176.

Ptacnik, R., Moorthi, S.D., Hillebrand, H., 2010. Hutchinson reversed, or why there need to be so many species. Advances in Ecological Research 43, 1–43.

Ptacnik, R., Solimini, A.G., Andersen, T., Tamminen, T., Brettum, P., Lepisto, L., Willén, E., Rekolainen, S., 2008. Diversity predicts stability and resource use efficiency in natural phytoplankton communities. In: Proceedings of the National Academy of Sciences of the United States of America, vol. 105, pp. 5134–5138.

Roy, S., Chattopadhyay, Y., 2007. Towards a resolution of 'the paradox of the plankton': a brief overview of proposed mechanisms. Ecological Complexity 4, 26–33.

Saiz, E., Kiørboe, T., 1995. Predatory and suspension feeding of the copepod *Acartia tonsa* in turbulent environments. Marine Ecology Progress Series 122, 147–158.

Schartau, M., Oschlies, A., 2003. Simultaneous data-based optimization of a 1D-ecosystem model at three locations in the North Atlantic: Part II – standing stocks and nitrogen fluxes. Journal of Marine Research 61, 795–821.

Sieracki, M., Verity, P., Stoecker, D., 1993. Plankton community response to sequential silicate and nitrate depletion during the 1989 North-Atlantic spring bloom. Deep-Sea Research Part II – Topical Studies In Oceanography 40, 213–225.

Smayda, T.J., 1970. The suspension and sinking of phytoplankton in the sea. Oceanography and Marine Biology: An Annual Review 8, 353–414.

Stirling, G., Wilsey, B., 2001. Empirical relationships between species richness, evenness, and proportional diversity. American Naturalist 158, 286–299.

Strom, S.L., Miller, C.B., Frost, B.W., 2000. What sets lower limits to phytoplankton stocks in high-nitrate, low-chlorophyll regions of the open Ocean? Marine Ecology Progress Series 193, 19–31.

Strom, S.L., Morello, T.A., 1988. Comparative growth rates and yields of ciliates and heterotrophic dinoflagellates. Journal of Plankton Research 20, 571–584.

Tilman, D., Lehman, C., Thomson, K., 1997. Plant diversity and ecosystem productivity: theoretical considerations. In: Proceedings of the National Academy of Sciences of the United States of America, vol. 94, pp. 1857–1861.

Tiselius, P., Jonsson, P.R., 1990. Foraging behaviour of six calanoid copepods: observations and hydrodynamic analysis. Marine Ecology Progress Series 66, 23–33.

Verity, P.G., Langdon, C., 1984. Relationships between lorica volume, carbon, nitrogen, and ATP content of tintinnids in Narragansett Bay. Journal of Plankton Research 6, 859–868.

Visser, A.W., 2001. Hydromechanical signals in the plankton. Marine Ecology Progress Series 222, 1–24.

Visser, A.W., 2007. Motility of zooplankton: fitness, foraging and predation. Journal of Plankton Research 29, 447–461.

Worm, B., Barbier, E.B., Beaumont, N., Duffy, J.E., Folke, C., Halpern, B.S., Jackson, J.B.C., Lotze, H.K., Micheli, F., Palumbi, S.R., Sala, E., Selkoe, K.A., Stachowicz, J.J., Watson, R., 2006. Impacts of biodiversity loss on Ocean ecosystem services. Science 314, 787–790.

Worm, B., Lotze, H., Hillebrand, H., Sommer, U., 2002. Consumer versus resource control of species diversity and ecosystem functioning. Nature 417, 848–851.

Wunsch, C., Heimbach, P., 2007. Practical global Oceanic state estimation. Physica D – Nonlinear Phenomena 230, 197–208.

Yachi, S., Loreau, M., 1999. Biodiversity and ecosystem productivity in a fluctuating environment: the insurance hypothesis. In: Proceedings of the National Academy of Sciences of the United States of America, vol. 96, pp. 1463–1468.

Yool, A., Popova, E.E., Anderson, T.R., 2011. MEDUSA: a new intermediate complexity plankton exosystem model for the global domain. Geoscientific Model Development 4, 381–417.